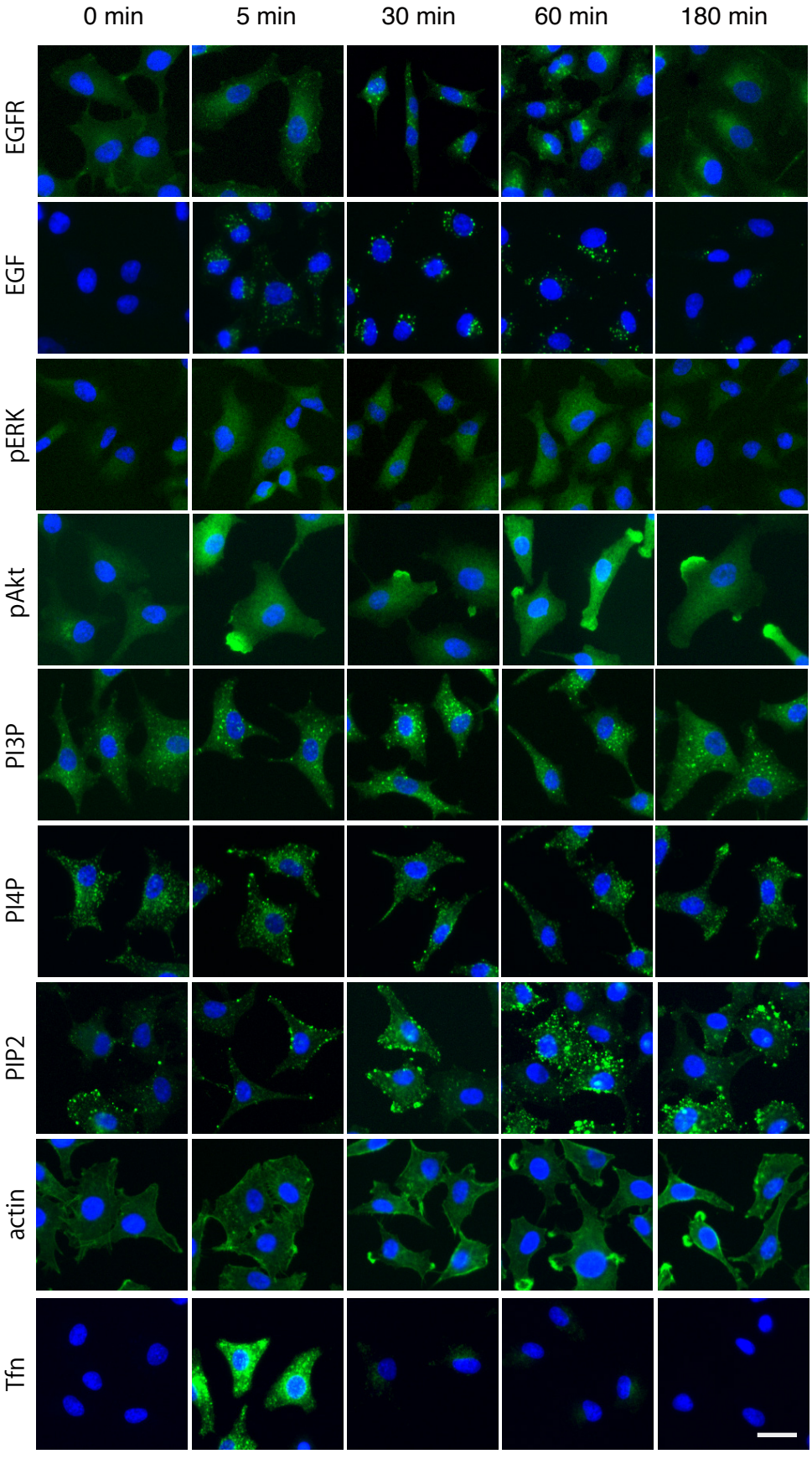

Supplementary Figure S1. Representative images of the EGF/EGFR time-course assay.

Cells were fixed at 0, 5, 30, 60, and 180 min after EGF stimulation and stained for EGFR, EGF, pERK, pAkt, PI3P, PI4P, PIP2, actin, and transferrin (Tfn). Columns indicate time after stimulation and rows indicate staining marker. Nuclei are stained with Hoechst (blue). Marker signals are displayed in green for visual consistency (pseudo-coloured where the original acquisition channel was not green). Scale bar, 20 μm.

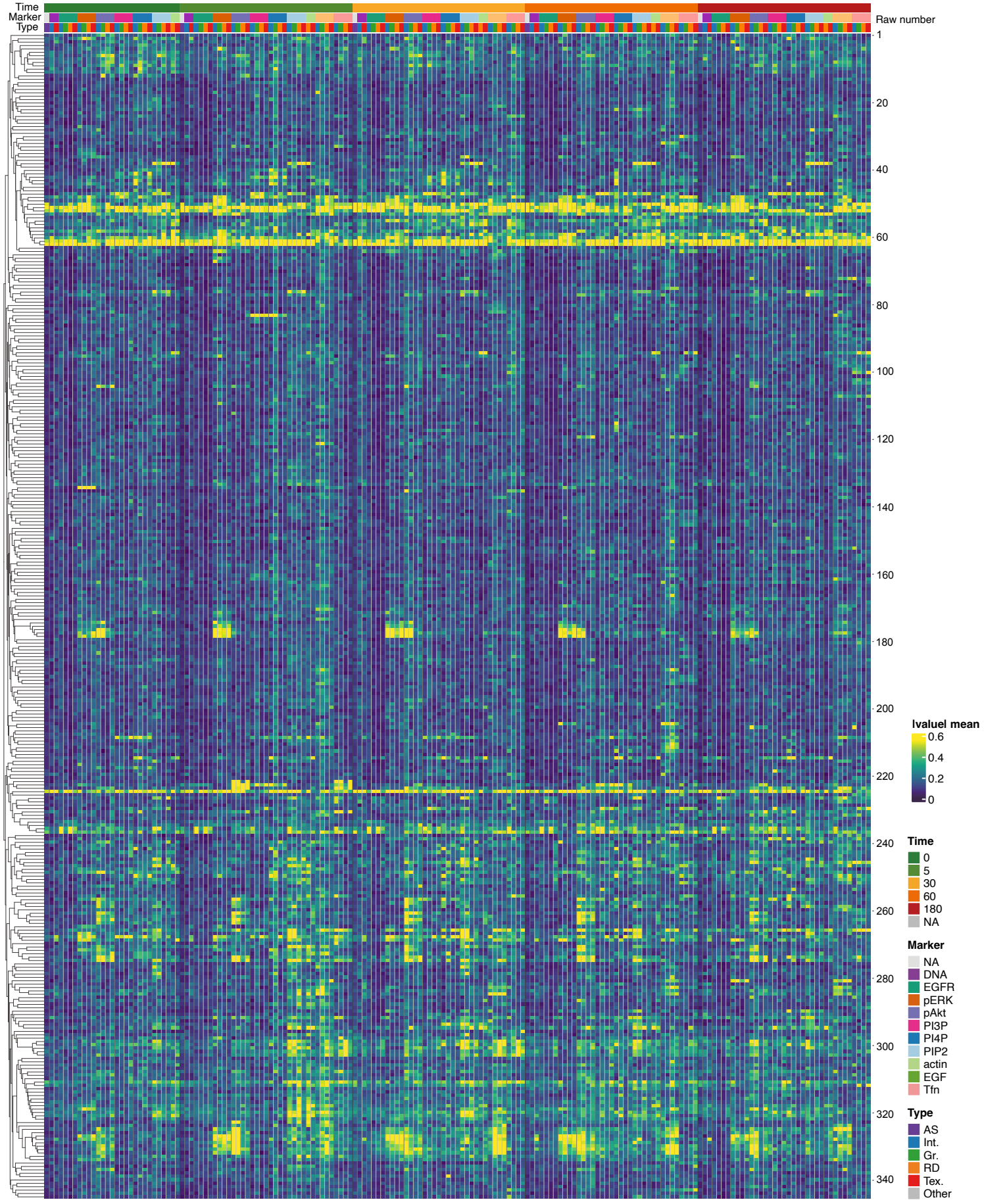

Tanabe Supplementary Fig. S2

Supplementary Figure S2. Global overview of compound clustering in the EGF/EGFR time-course assay.

Hierarchical clustering of compounds profiled by high-content screening (HCS) across the EGF/EGFR time course. Rows indicate compounds and columns indicate image features grouped by time point, staining marker, and feature type. For visualization, features were aggregated within each time × marker × type stratum as the mean absolute signed EMD relative to DMSO (mean |signed EMD|; "|value| mean"). Clustering was performed on the original (non-aggregated) signed-EMD feature matrix after removing highly correlated features (Pearson $|r| \geq 0.95$), using correlation distance with average linkage. This heatmap provides the full-library context corresponding to the clustered heatmaps shown in Fig. 3A and Fig. 4A. Feature-type abbreviations: AS, AreaShape; Int., Intensity; Gr., Granularity; RD, RadialDistribution; Tex., Texture. Compound names are listed in Supplementary Table S17; "Raw number" is provided to facilitate matching to the Raw number field in Supplementary Table S17.

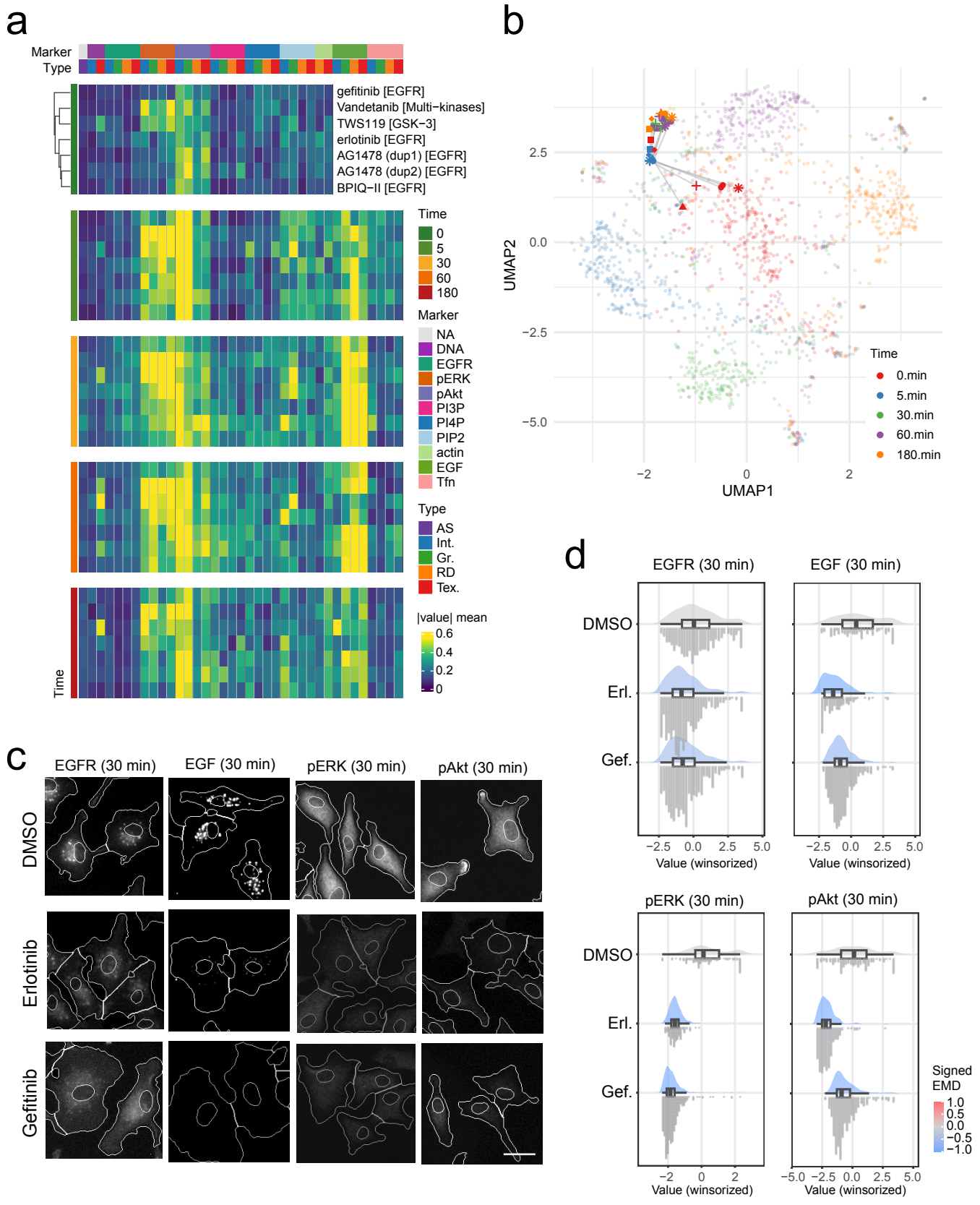

Supplementary Figure S3. EGFR inhibitors define a coherent phenotype in the EGFR time-course assay.

(a) Heatmap summary of time-resolved marker signatures for representative EGFR-pathway inhibitors and comparators; annotations denote time, marker, feature type, and the mean |signed EMD| scale. (b) UMAP (as in Fig. 2A) highlighting EGFR inhibitor trajectories (arrows) across time. (c) Representative single-marker images at 30 min for EGFR, EGF, pERK, and pAkt under DMSO, erlotinib, or gefitinib treatment. Scale bar, 20 μm. (d) Raincloud plots summarising signed EMD distributions for EGFR, EGF, pERK, and pAkt at 30 min (colour indicates signed EMD as shown).

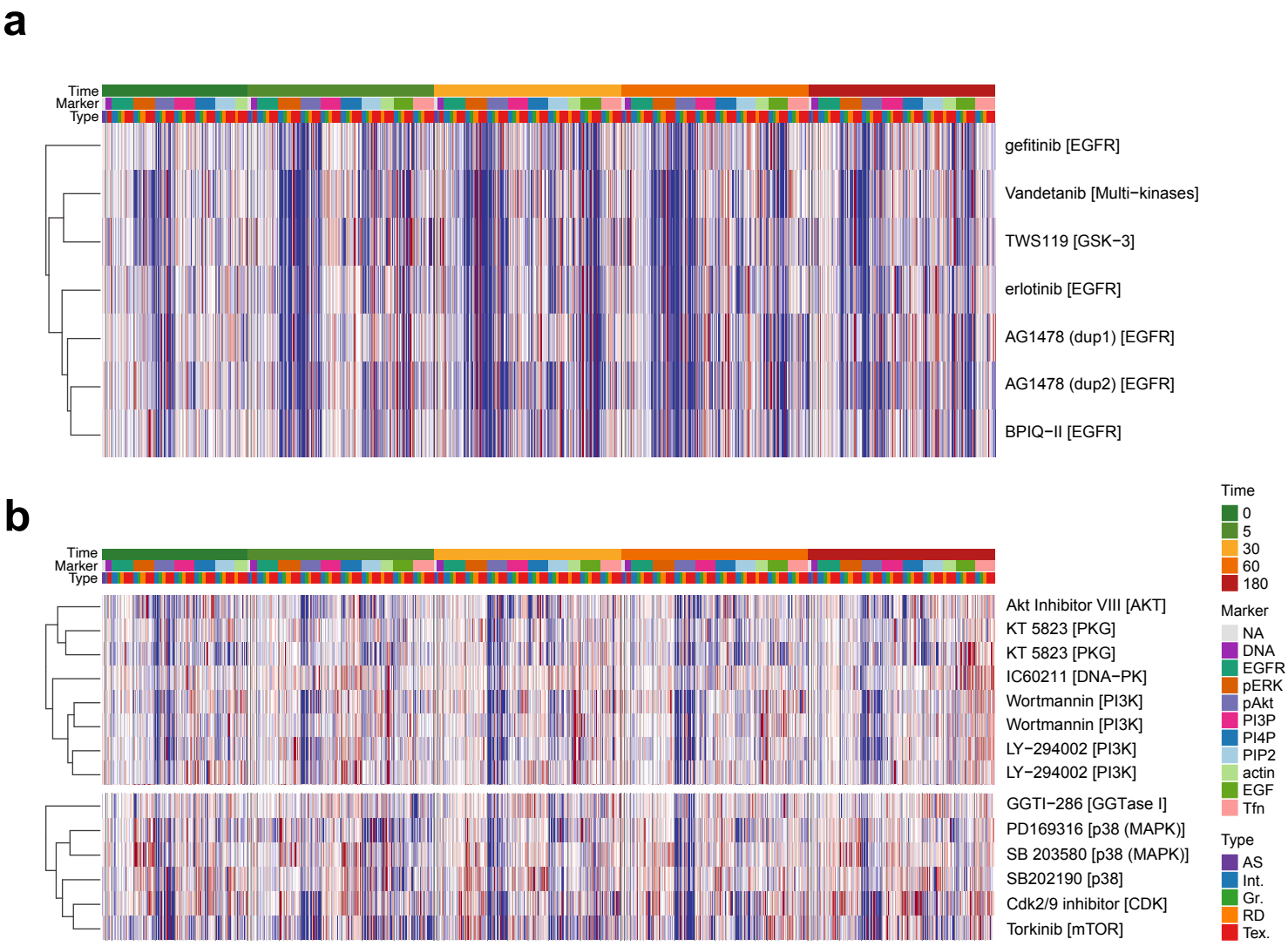

Supplementary Figure S4. Signed (non-aggregated) heatmaps for the EGFR-inhibitor and PI3K-inhibitor clusters.

Heatmaps of the original, non-aggregated signed-EMD features (relative to DMSO) for the two clusters highlighted in Fig. 3 and Fig. 4. (a) Cluster containing EGFR/ERBB-pathway inhibitors. (b) Cluster containing PI3K inhibitors. Columns are ordered by time point, staining marker, and feature type as in Supplementary Fig. S2. Unlike the aggregated display in Fig. 3A/4A and Fig. S2, these panels retain the sign of the response, revealing directionality of feature changes (e.g., broadly negative responses in panel A and prominent negative pAkt-associated features in panel B). Feature-type abbreviations are as in Supplementary Fig. S2.

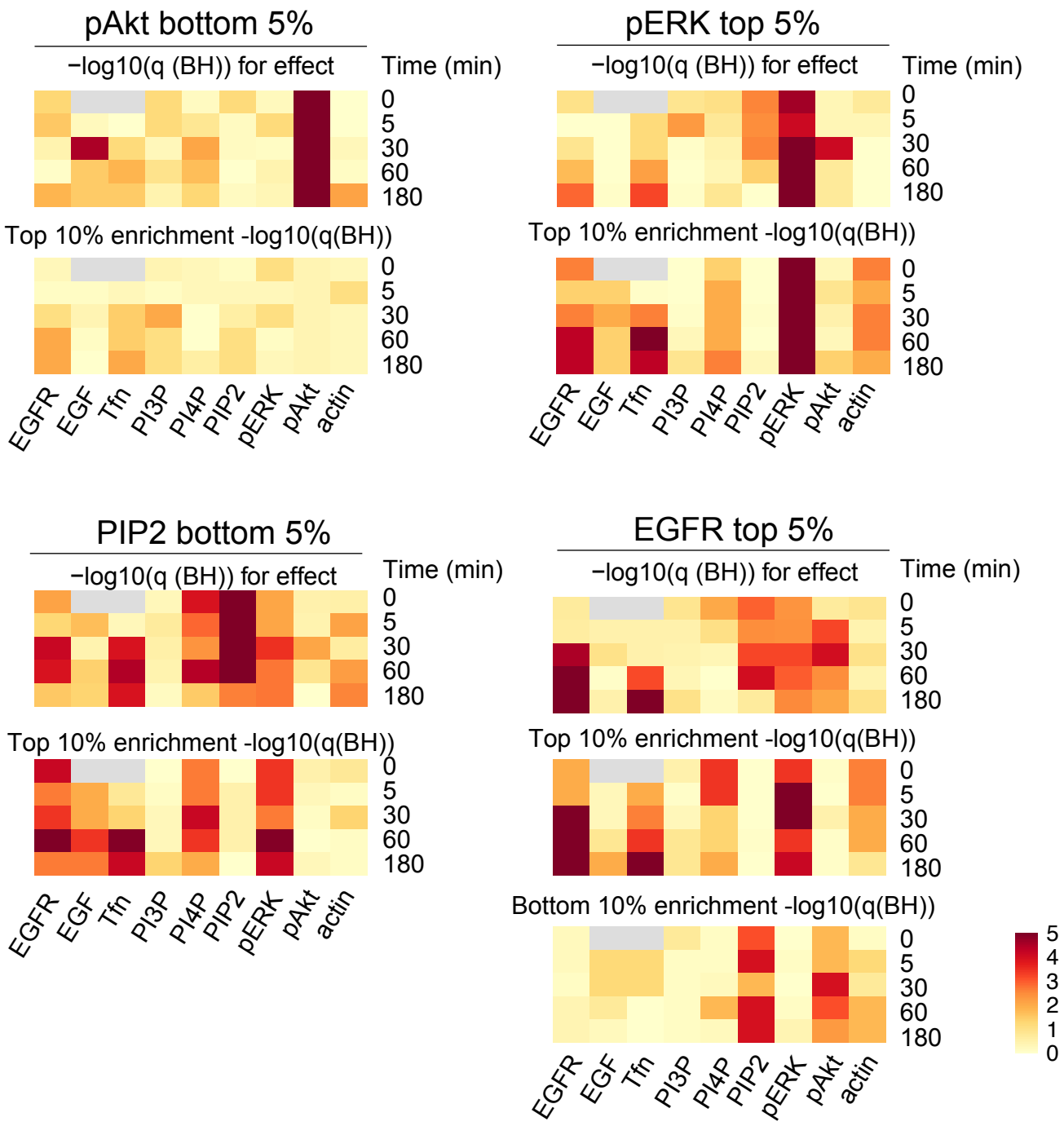

Supplementary Figure S5. Significance maps corresponding to Fig. 3E.

Heatmaps report the statistical significance for the marker–time signatures shown in Fig. 3E, displayed as −log10(q) after Benjamini–Hochberg (BH) correction. Panels correspond to compound groups selected as in Fig. 3E (pAkt bottom 5% at 30 min; pERK top 5% at 30 min; PIP2 bottom 5% at 30 min; EGFR granularity top 5% at 180 min). For each group, the upper heatmap shows −log10 (q(BH)) from the Wilcoxon rank-sum test for the effect-size comparison (selected vs non-selected) at each marker and time point. The lower heatmaps show −log10(q(BH)) from Fisher's exact test for enrichment of the selected group within distribution tails (top 10% tail for all groups; for the EGFR-selected group, enrichment in the bottom 10% tail is also shown). Larger values indicate stronger statistical support. These panels report q-value significance maps and are shown separately from the outline encodings used in the corresponding effect/enrichment summaries.

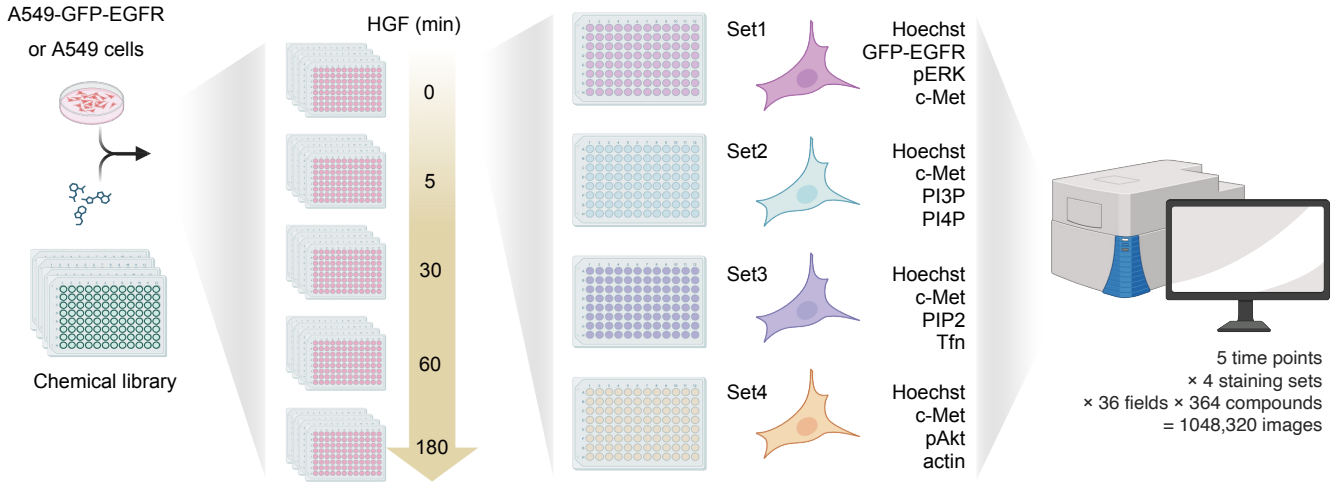

Supplementary Figure S6. Workflow for the HGF/c-Met time-course assay.

Schematic of the experimental workflow for the HGF/c-Met time-course imaging assay (HGF counterpart of Fig. 1A, excluding the Cell Painting arm). Cells were treated with the chemical library and stimulated with HGF, then fixed at 0, 5, 30, 60, and 180 min. Set 1 was performed in A549 cells stably expressing GFP–EGFR, whereas sets 2–4 were performed in parental A549 cells. Cells were immunostained and imaged in four staining sets: set 1, Hoechst, GFP–EGFR, phospho-ERK (pERK), and c-Met; set 2, Hoechst, PI4P, c-Met, and PI3P; set 3, Hoechst, PI(4,5)P_2 (PIP_2), c-Met, and Alexa Fluor 647–conjugated transferrin (Tfn); and set 4, Hoechst, F-actin, phospho-Akt (pAkt), and c-Met. Images were acquired by automated fluorescence microscopy (5 time points × 4 staining sets; 36 fields × 364 compounds; total 1,036,800 images).

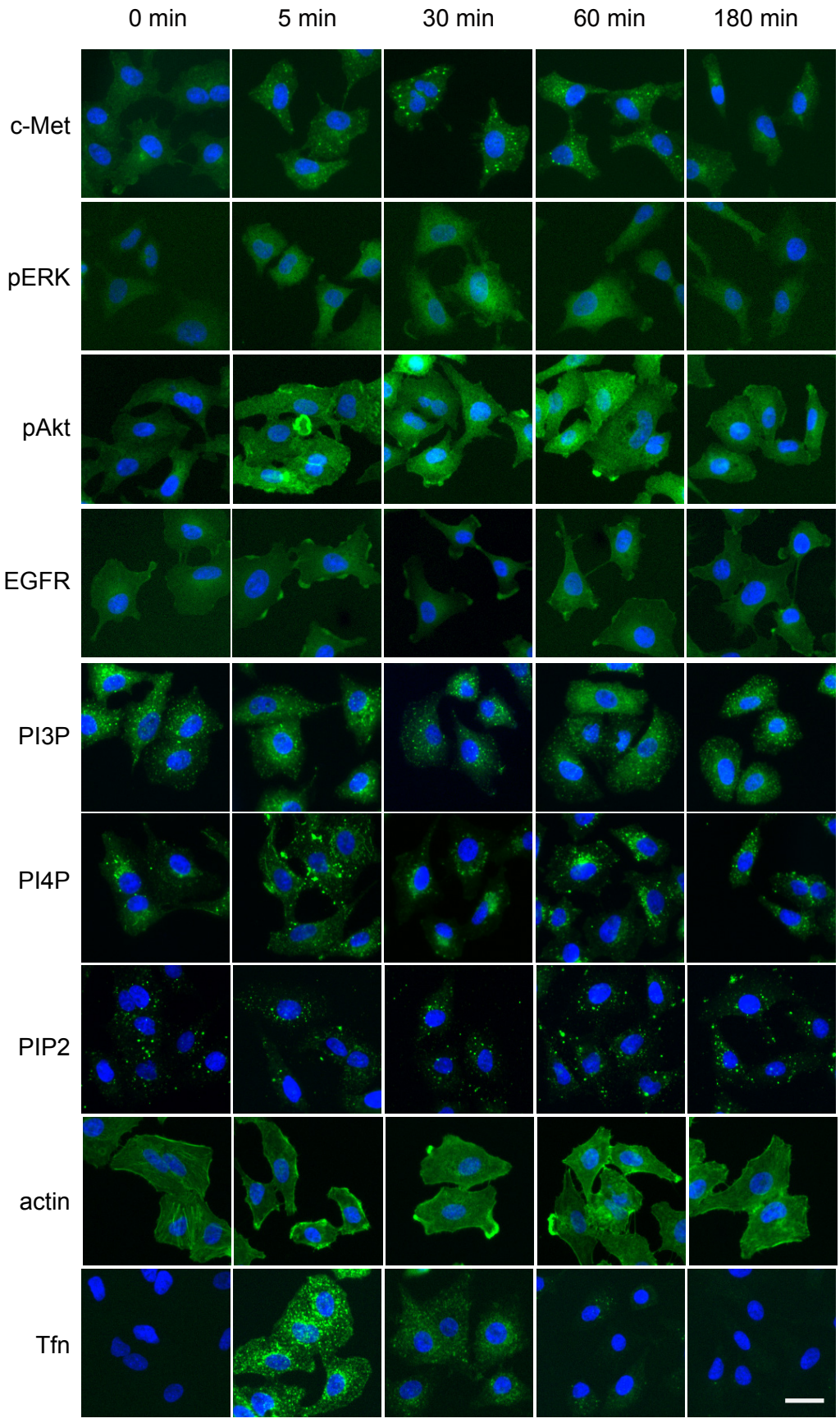

Supplementary Figure S7. Representative images of the HGF/c-Met time-course assay.
Representative images for the HGF/c-Met time-course assay (HGF counterpart of Supplementary Fig. S1). Cells were fixed at 0, 5, 30, 60, and 180 min after HGF stimulation and stained for c-Met, pERK, pAkt, EGFR, PI3P, PI4P, PIP2, actin, and transferrin (Tfn). Columns indicate time after stimulation and rows indicate staining marker. Nuclei are stained with Hoechst (blue). Marker signals are displayed in green for visual consistency (pseudo-coloured where the original acquisition channel was not green). Scale bar, 20 μm.

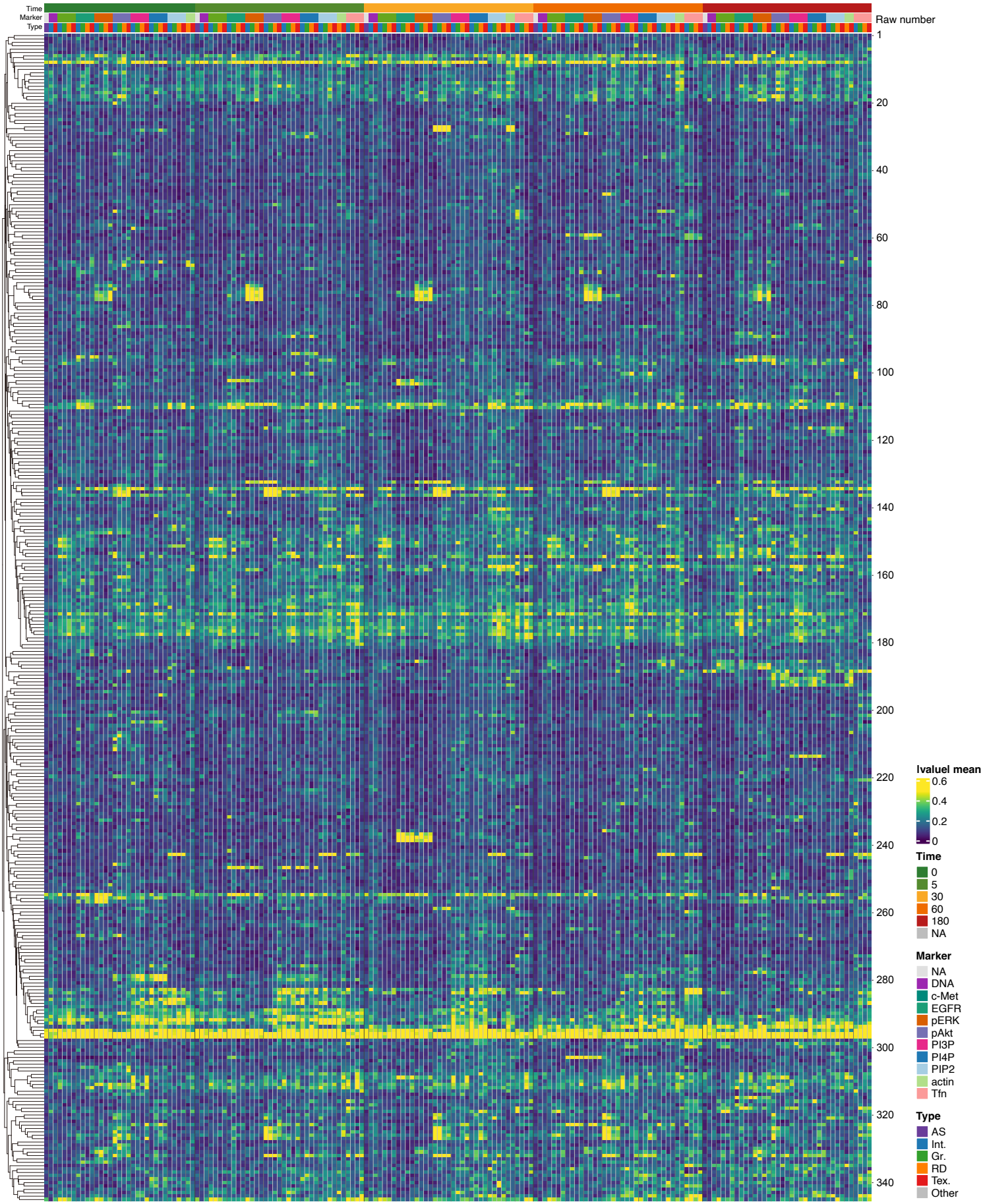

Tanabe Supplementary Fig. S8

Supplementary Figure S8. Global overview of compound clustering in the HGF/c-Met time-course assay.

Hierarchical clustering of compounds profiled by high-content screening (HCS) across the HGF/c-Met time course. Rows indicate compounds and columns indicate image features grouped by time point, staining marker, and feature type. For visualization, features were aggregated within each time × marker × type stratum as the mean absolute signed EMD relative to DMSO (mean |signed EMD|; "|value| mean"). Clustering was performed on the original (non-aggregated) signed-EMD feature matrix after removing highly correlated features (Pearson $|r| \geq 0.95$), using correlation distance with average linkage. This heatmap provides the full-library context for the HGF/c-Met dataset. Feature-type abbreviations: AS, AreaShape; Int., Intensity; Gr., Granularity; RD, RadialDistribution; Tex., Texture. Compound names are listed in Supplementary Table S18; "Raw number" is provided to facilitate matching to the Raw number field in Supplementary Table S18.

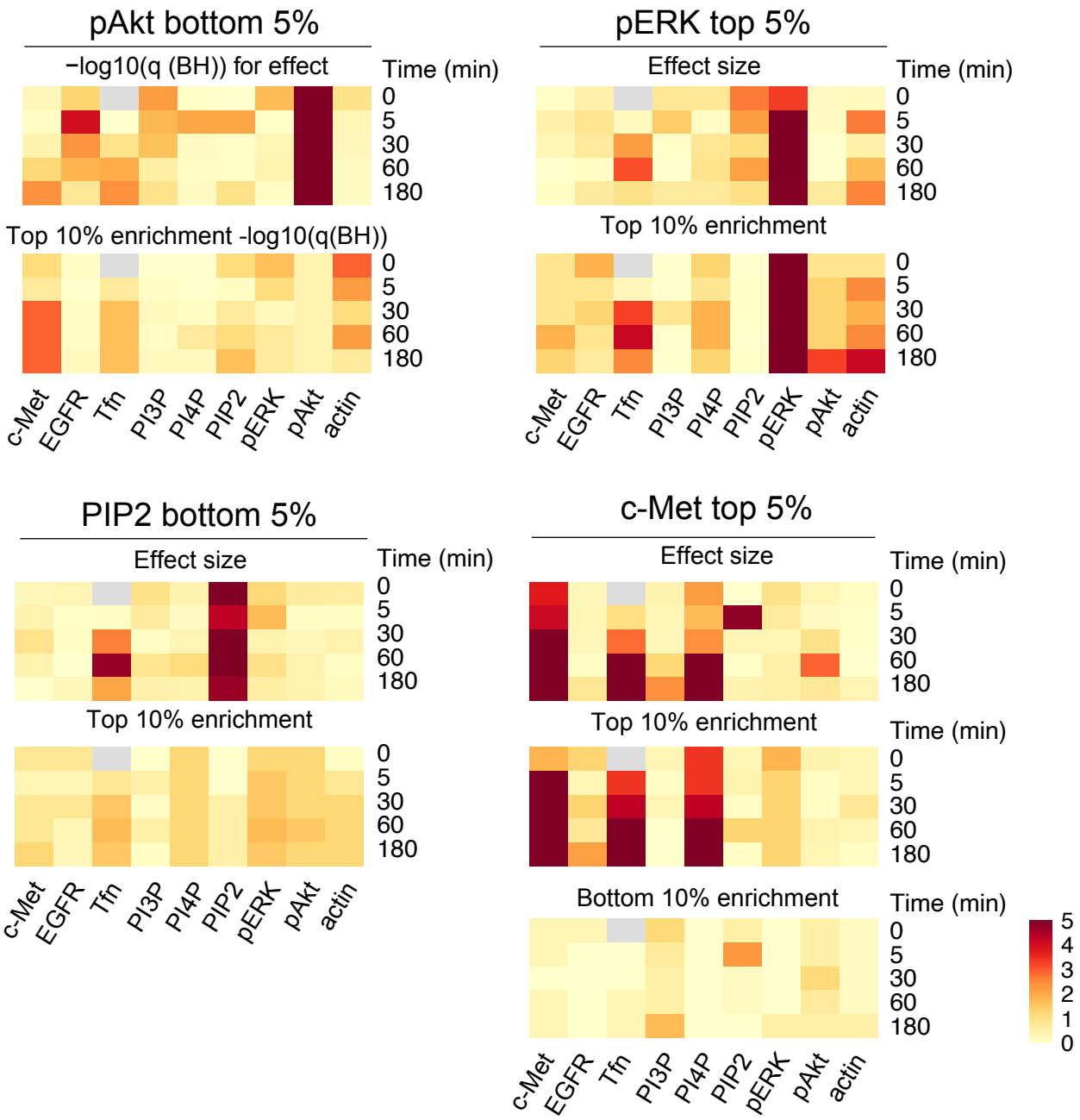

Supplementary Figure S9. Significance maps corresponding to Fig. 4E.

Heatmaps report the statistical significance for the marker–time signatures shown in Fig. 4e, displayed as −log10(q) after Benjamini–Hochberg (BH) correction. Compound groups were selected as in Fig. 3e (pAkt bottom 5% at 30 min; pERK top 5% at 30 min; PIP2 bottom 5% at 30 min; c-Met top 5% at 180 min). For each group, the upper heatmap shows −log10(q(BH)) from the Wilcoxon rank-sum test for the effect-size comparison (selected vs non-selected) at each marker and time point. The lower heatmaps show −log10(q(BH)) from Fisher's exact test for enrichment of the selected group within distribution tails (top 10% tail; for the c-Met–selected group, enrichment in the bottom 10% tail is also shown as indicated). Larger values indicate stronger statistical support. These panels report q-value significance maps and are shown separately from the outline encodings used in the corresponding effect/enrichment summaries.

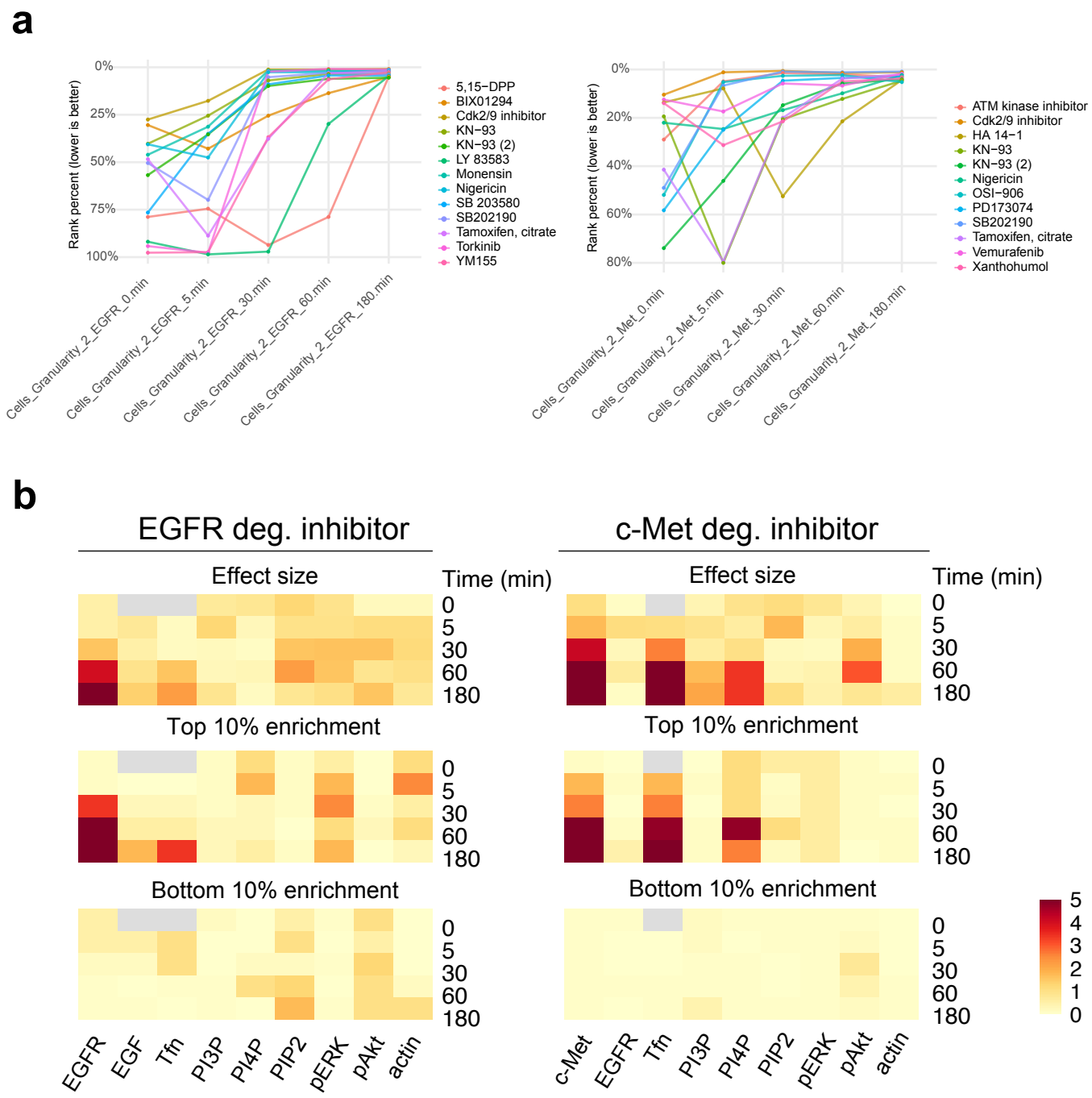

Supplementary Figure S10. Per-compound granularity rank trajectories and corresponding significance maps for receptor degradation-inhibitor groups.

(a) Compound-level “bump plots” underlying Fig. 5a. Each line represents a single compound in the empirically defined degradation-inhibitor groups, plotted as rank percent of receptor granularity across the 0–180 min time course (lower rank percent indicates higher granularity). Left, EGFR degradation-inhibitor group; right, c-Met degradation-inhibitor group.

(b) Heatmaps reporting the significance of the group signatures shown in Fig. 5c (same group order as in A). Values are shown as −log10(q) after Benjamini–Hochberg (BH) correction. The upper block corresponds to effect-size comparisons (Δmean signed EMD; selected vs non-selected; Wilcoxon rank-sum test), and the middle and lower blocks correspond to enrichment within the top and bottom 10% distribution tails, respectively ($\log_2$ enrichment; Fisher’s exact test).

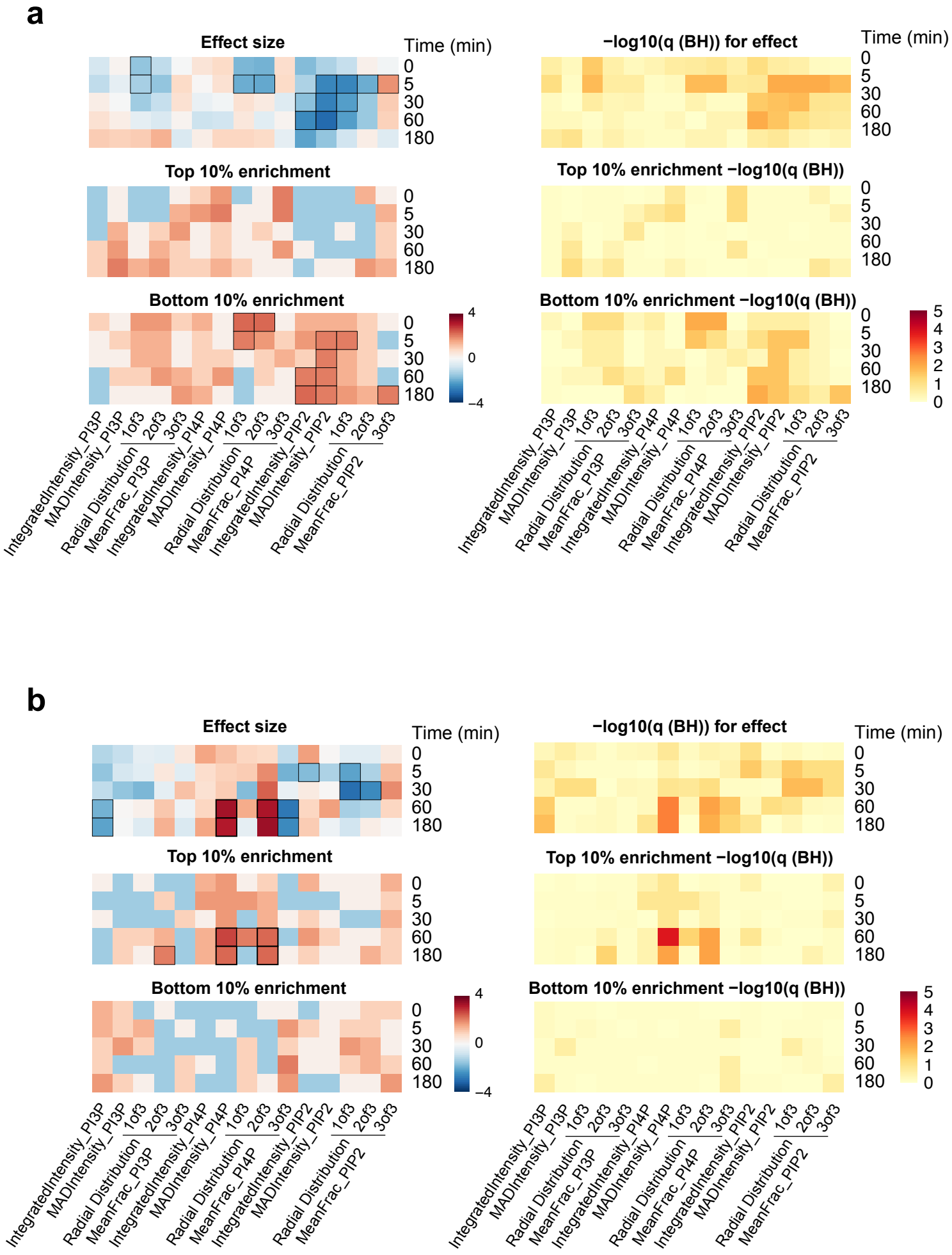

Tanabe Supplementary Fig. S11

Supplementary Figure S11. Lipid-marker signatures in receptor degradation-inhibitor groups.

Heatmap summary of statistical results for the lipid markers PI3P, PI4P, and PIP2 using their major representative features (integrated intensity, MAD intensity, and radial-distribution features). (a) EGFR degradation inhibitors and (b) c-Met degradation inhibitors, defined as in Fig. 5. For each group, the left panels show (top) effect size (Δmean signed EMD; selected vs non-selected), (middle) top-10% tail enrichment (log_2 enrichment of the selected group within the top 10% of the marker/time distribution), and (bottom) bottom-10% tail enrichment (log_2 enrichment within the bottom 10% tail), across the 0–180 min time course. Radial-distribution features are shown as MeanFrac measured at three radial bins (1/3, 2/3, 3/3). Thin black outlines indicate BH-adjusted $q < 0.05$ and thick black outlines indicate BH-adjusted $q < 0.01$ (q values are Benjamini–Hochberg–adjusted for the corresponding test as described). The right panels report the corresponding statistical significance as $-\log10(q(BH))$ for each heatmap (Wilcoxon rank-sum test with BH correction for effect sizes; Fisher's exact test with BH correction for enrichment).

a

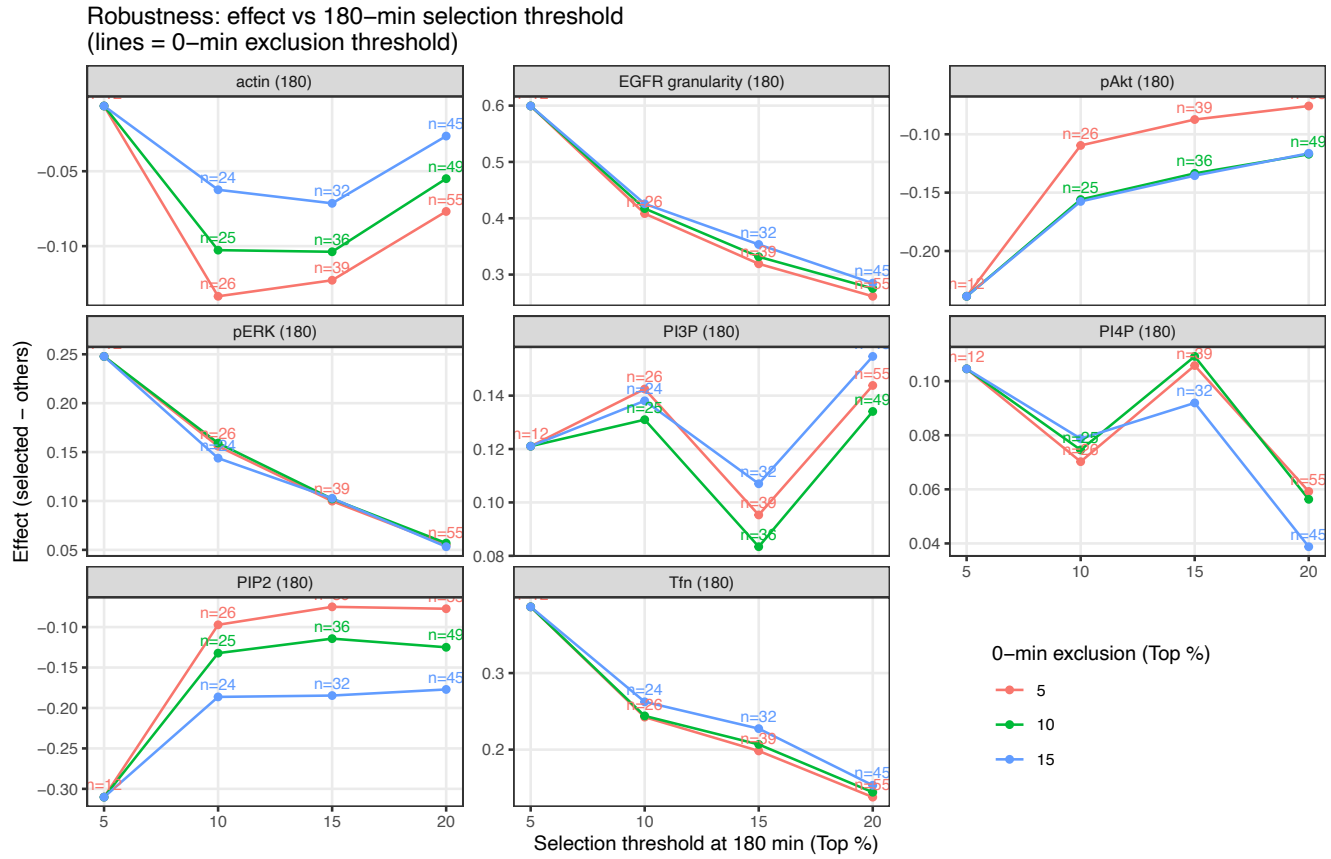

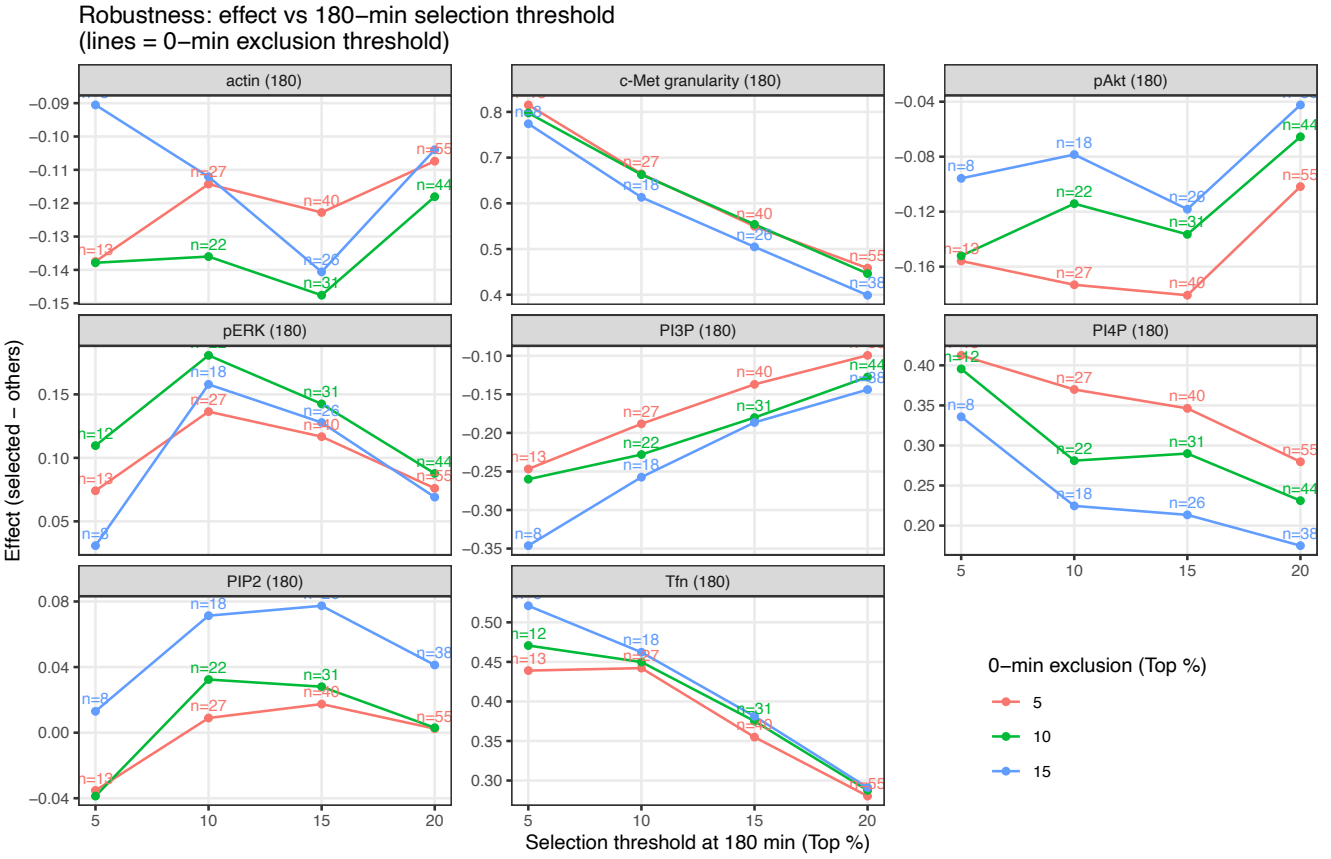

Tanabe Supplementary Fig. S12

b

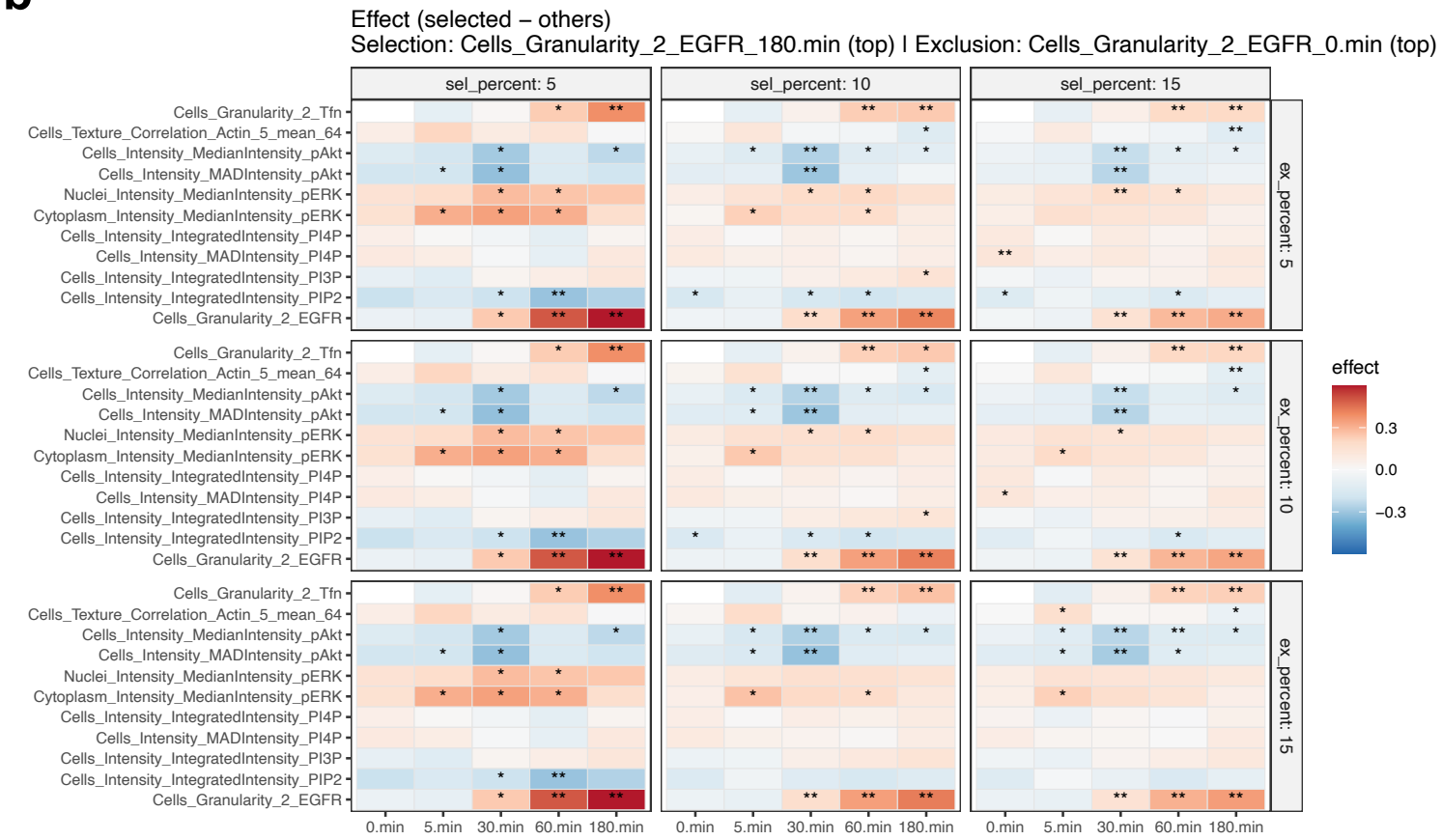

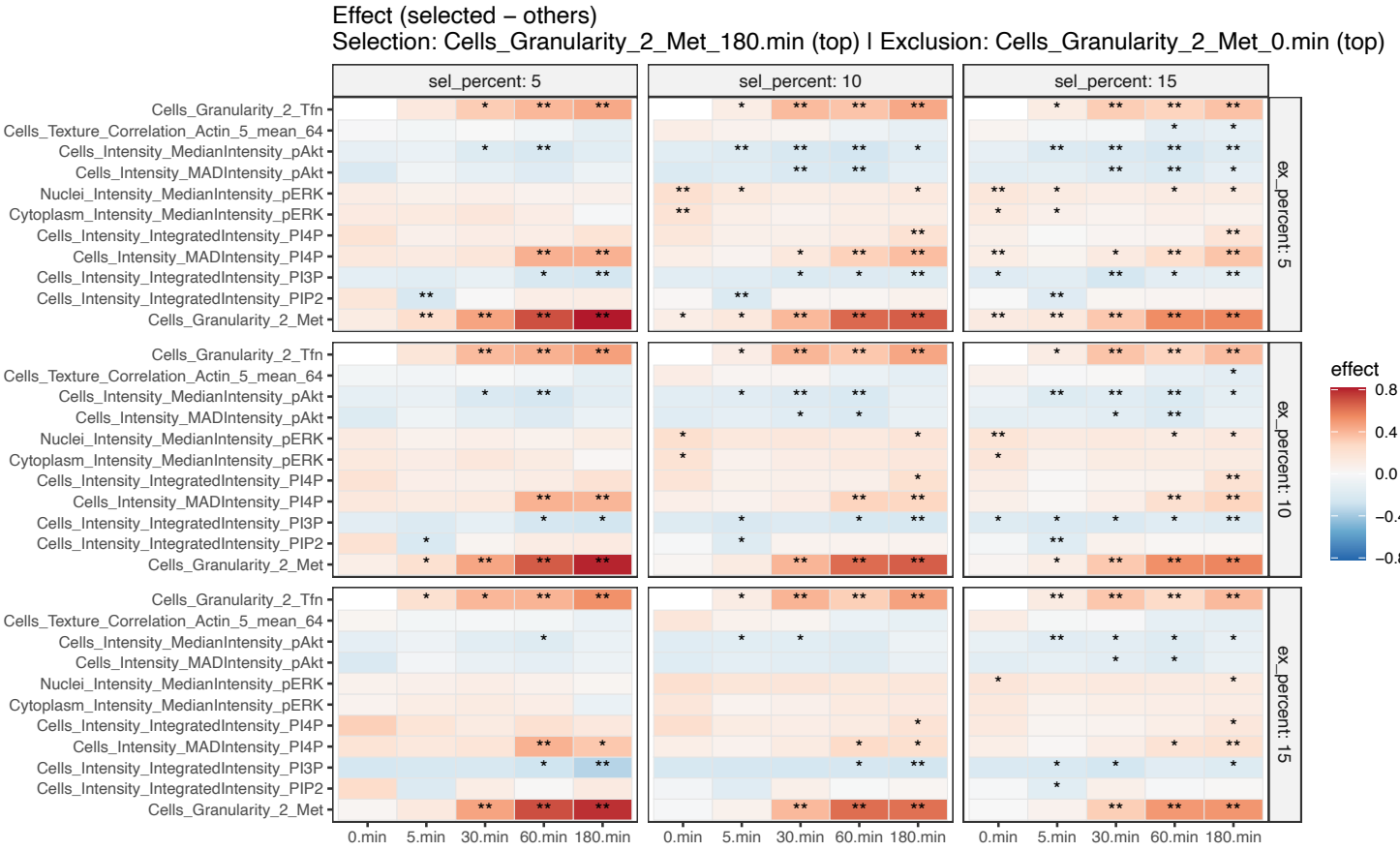

Tanabe Supplementary Fig. S12

c

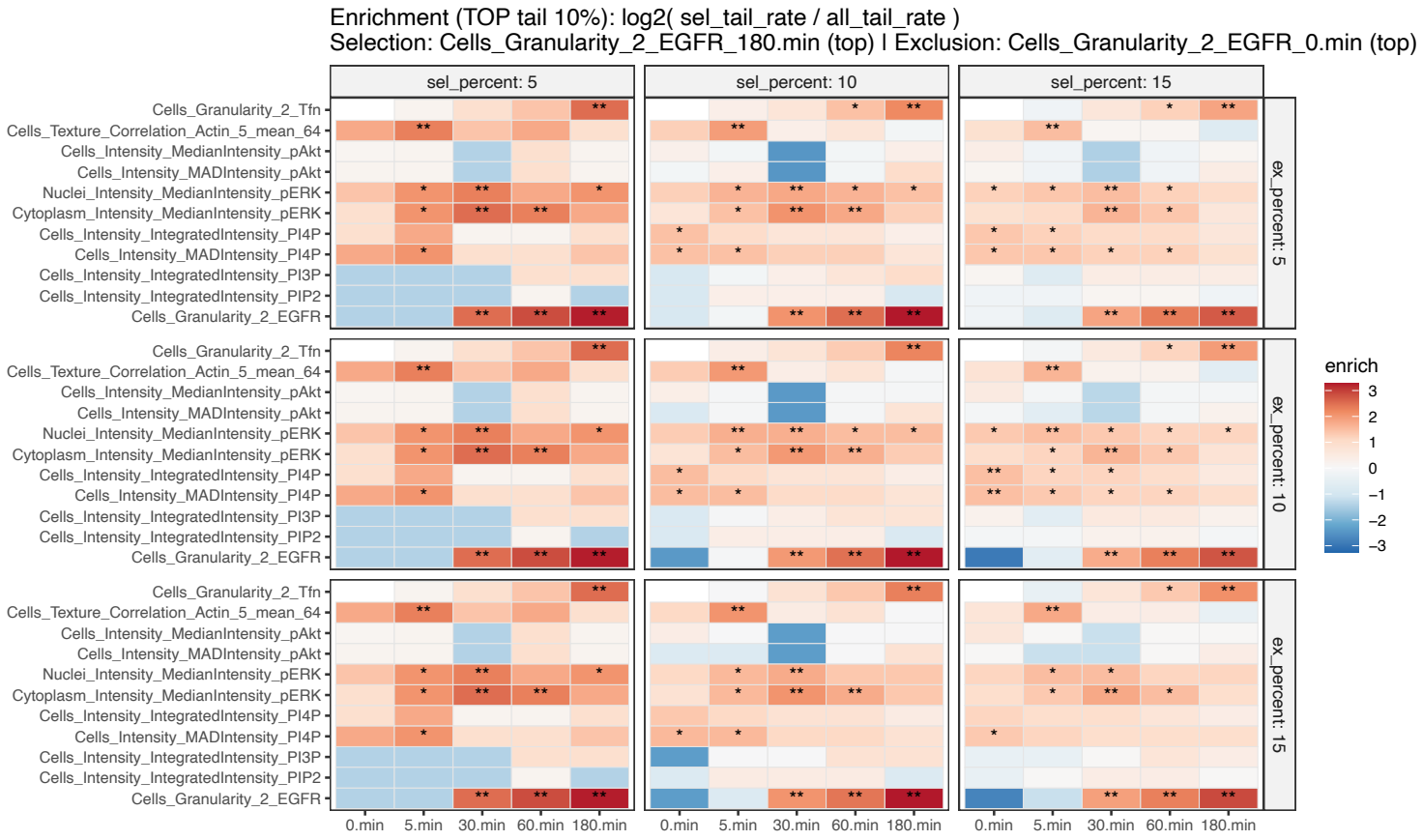

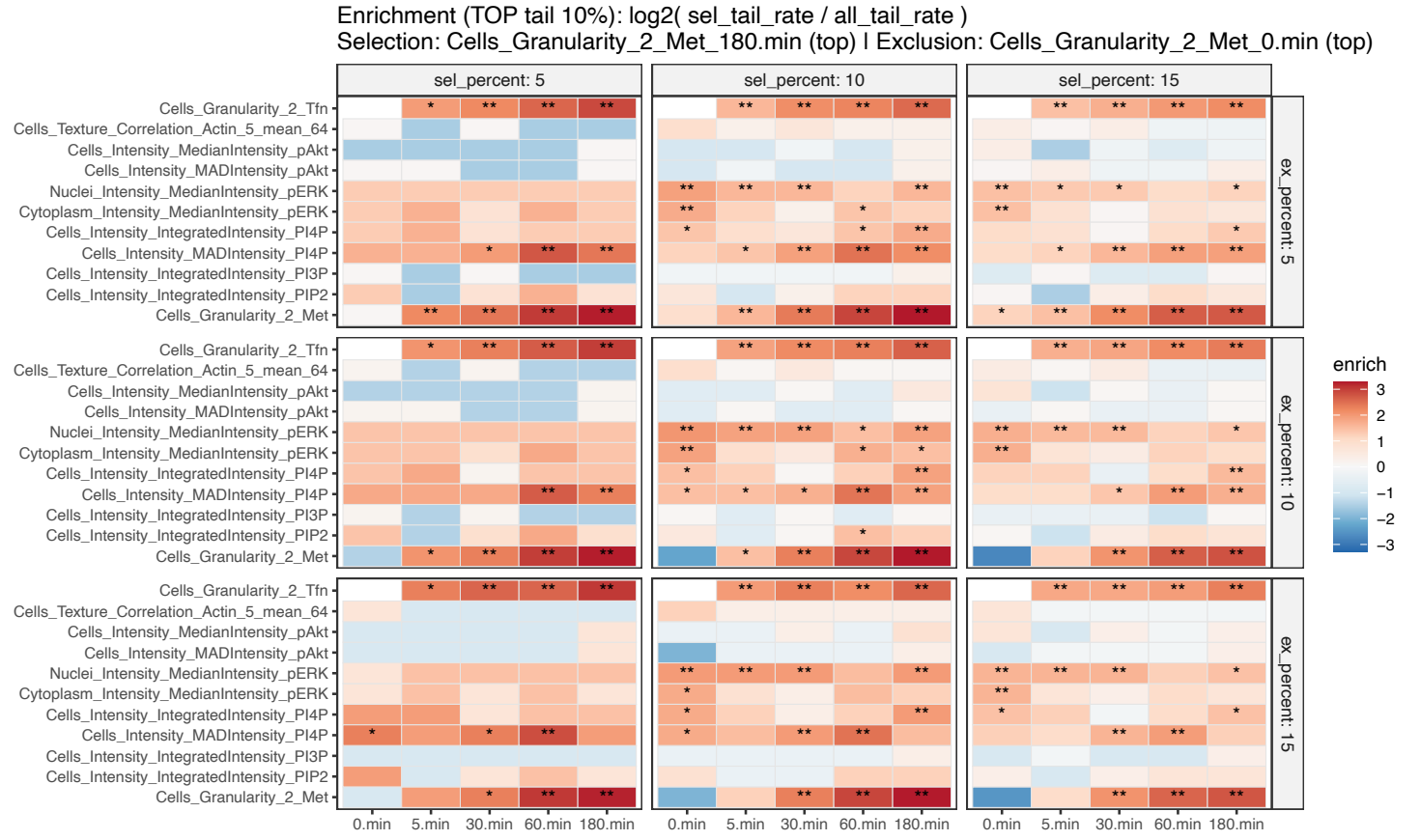

Tanabe Supplementary Fig. S12

d

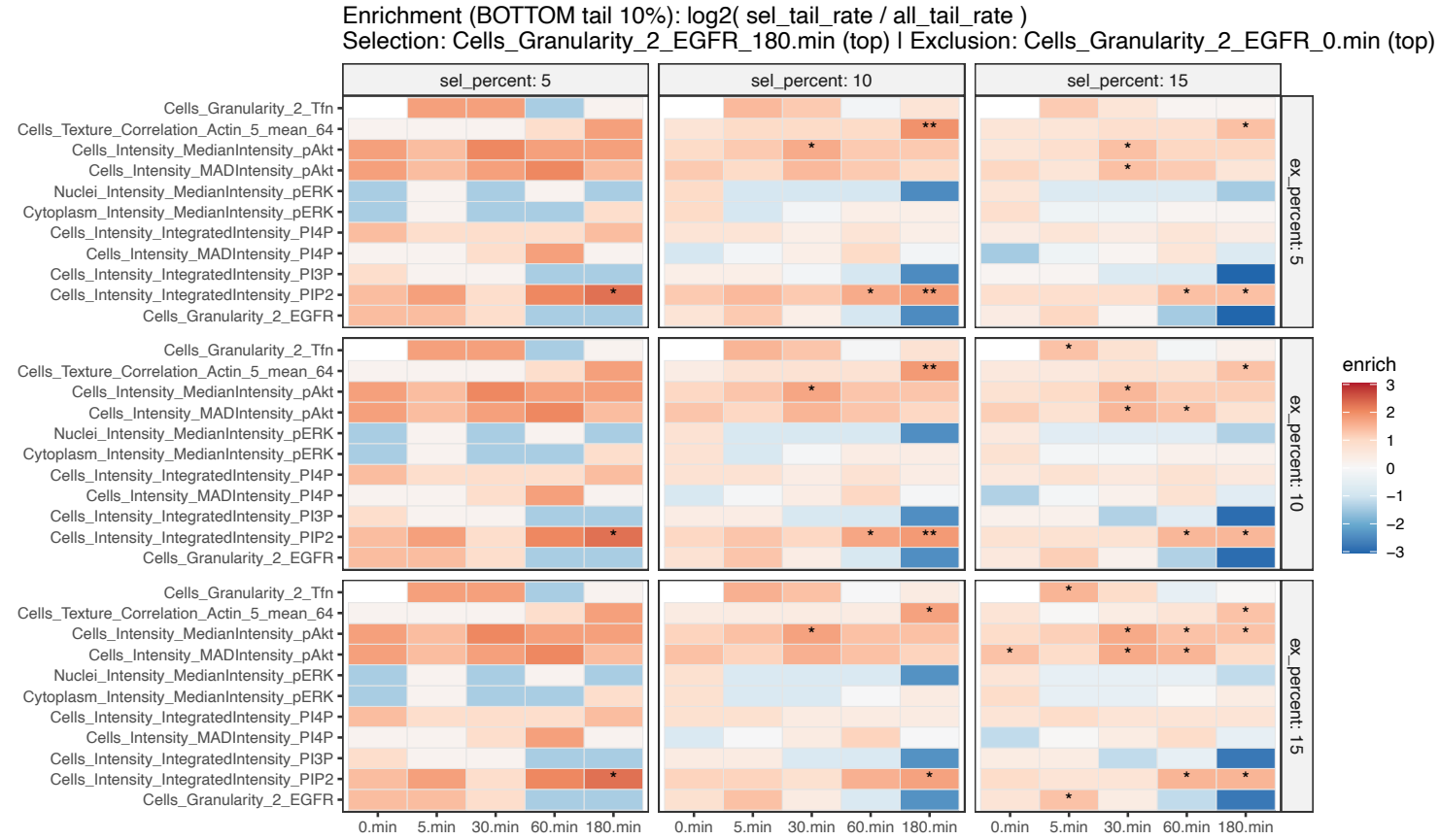

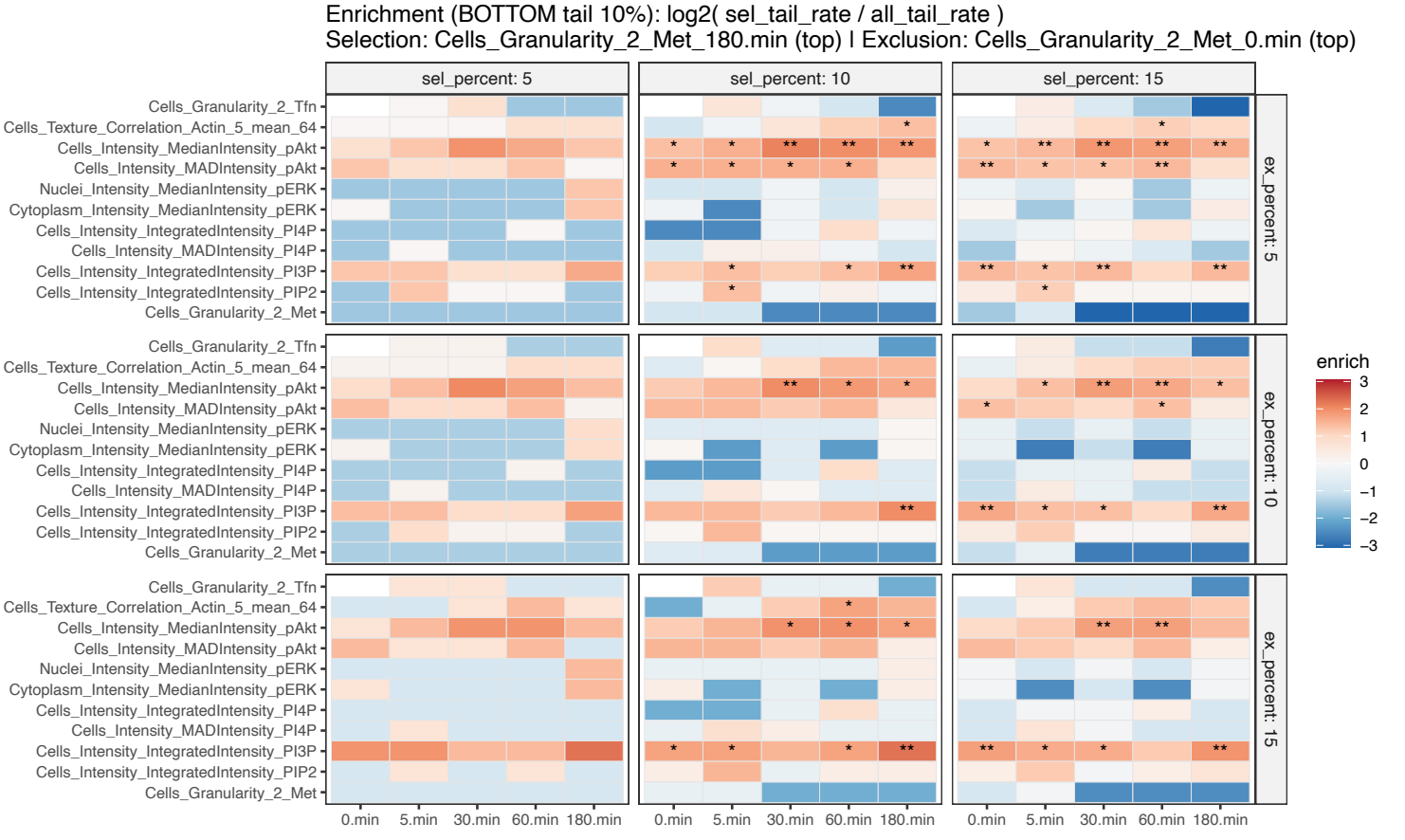

Tanabe Supplementary Fig. S12

Supplementary Figure S12. Robustness of Fig. 5c signatures to selection-stringency thresholds.

To assess how the conclusions in Fig. 5c depend on the empirical definition of "degradation-inhibitor" groups, we repeated the analyses while varying (i) the selection threshold at 180 min (top-ranked receptor-granularity wells; x-axis / column facet) and (ii) the 0-min exclusion threshold used to remove high-basal granularity phenotypes (top-ranked at 0 min; line colour / row facet). In all panels, the upper block shows the EGFR-based selection and the lower block shows the c-Met–based selection.

(a) Effect-size robustness at 180 min. For the indicated readouts (actin, receptor granularity, pERK, PI4P, PIP2, and Tfn at 180 min), curves show the effect size (Δmean signed EMD; selected − others) as a function of the 180-min selection threshold; line colours indicate the 0-min exclusion threshold. Numbers adjacent to points indicate the number of selected compounds.

(b) Effect-size heatmaps across the full time course (0–180 min) for representative marker features (same definition as in Fig. 5c). Heatmaps show Δmean signed EMD (selected − others) for each time point and marker feature under each combination of thresholds (columns: 180-min selection stringency; rows: 0-min exclusion stringency). Significance is assessed by a Wilcoxon rank-sum test with BH correction and overlaid as symbols ($q < 0.05$ / $q < 0.01$).

(c–d) Enrichment robustness in distribution tails. Heatmaps show $\log_2$ enrichment of the selected group within the top 10% tail (c) or bottom 10% tail (d) of each marker/time distribution, computed as $\log_2$(sel_tail_rate / all_tail_rate). Significance is assessed by Fisher's exact test with BH correction and overlaid as symbols ($q < 0.05$ / $q < 0.01$).

a

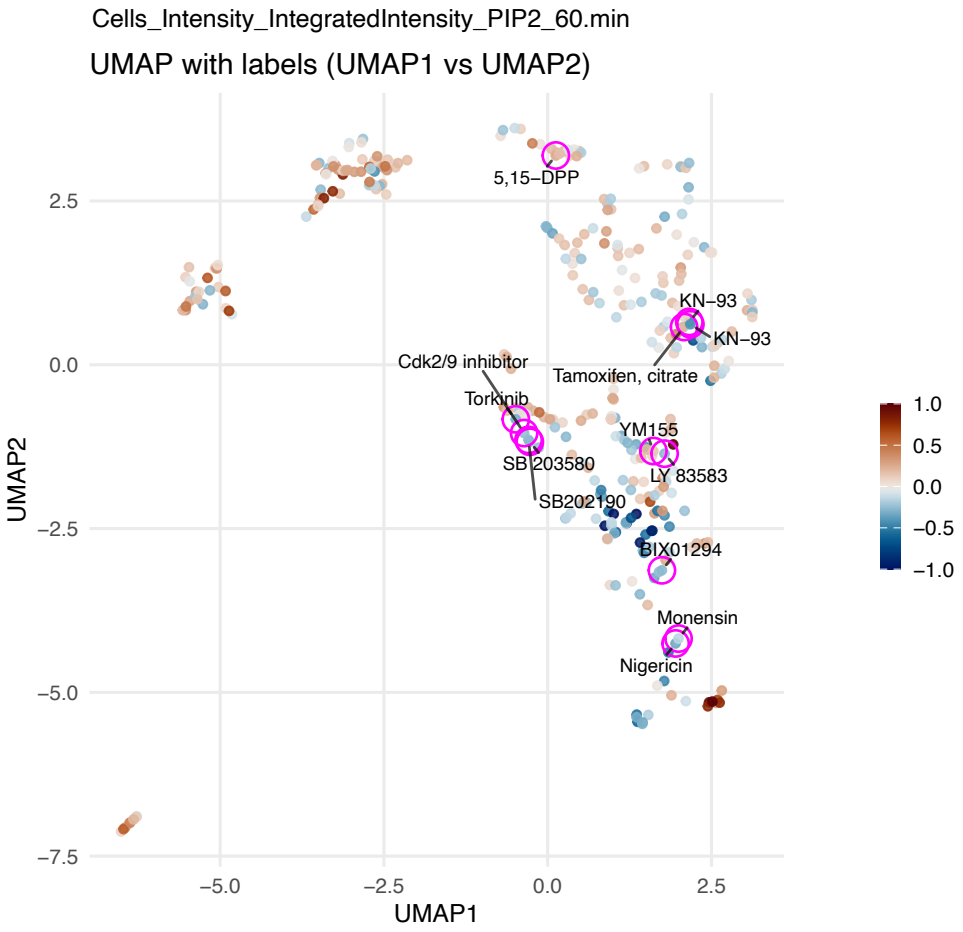

b

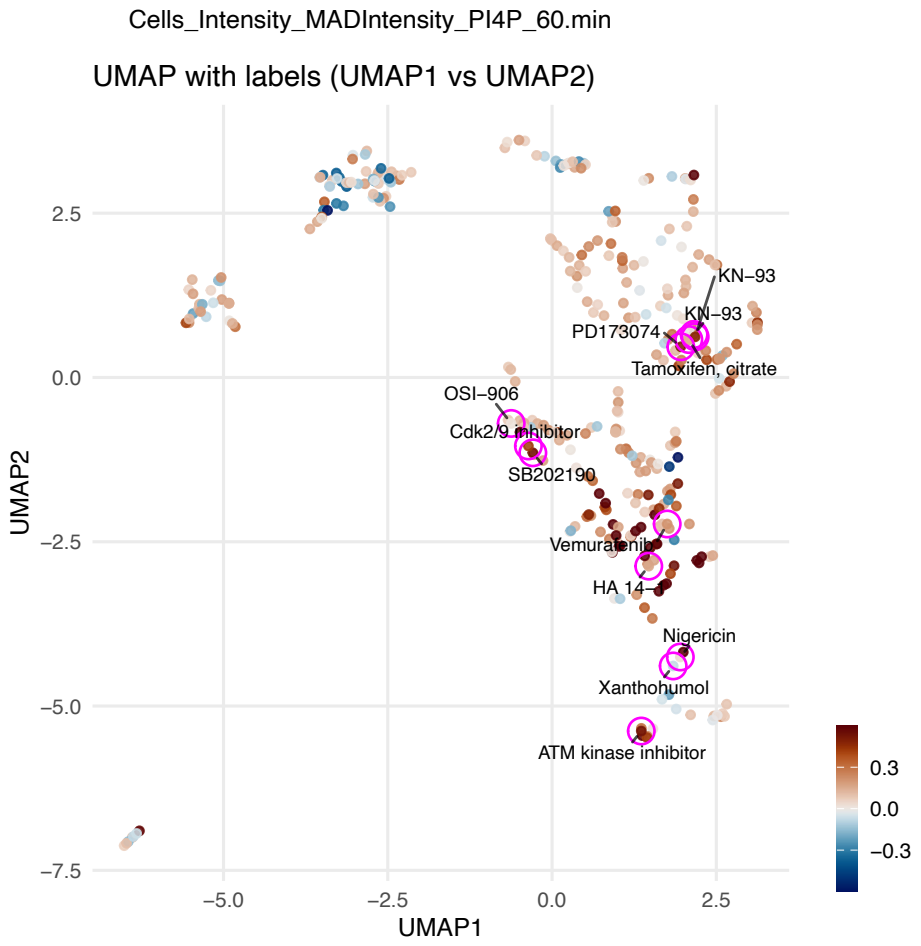

Tanabe Supplementary Fig. S13

Supplementary Figure S13. Lipid-feature gradients on the fused UMAP and locations of receptor degradation inhibitors.

Wells are shown in the fused UMAP embedding from Fig. 6a (UMAP1 vs UMAP2) and coloured by representative lipid-marker feature values at 60 min. (a) Cells_Intensity_IntegratedIntensity _PIP2_60.min. (b) Cells_Intensity_MADIntensity_PI4P_60.min. Circles highlight wells corresponding to the receptor degradation-inhibitor groups defined as in Fig. 5 (EGFR group in a; c-Met group in b).